

CLIC PHYSICS STUDY GROUP

## Physics Signatures at CLIC

Marco Battaglia  
CERN - PS Division

### Abstract

A set of signatures for physics processes of potential interests for the CLIC programme at  $\sqrt{s} = 1 - 5$  TeV are discussed. These signatures, that may correspond to the manifestation of different scenarios of new physics as well to Standard Model precision tests, are proposed as benchmarks for the optimisation of the CLIC accelerator parameters and for a first definition of the required detector response.

Based on material presented at the  
1<sup>st</sup> Open Meeting for CLIC Physics Studies  
CERN, 25 - 26 May, 2000

Geneva, Switzerland  
31 January, 2001

# 1 Introduction

The CLIC concept aims for a linear collider providing collisions at centre-of-mass energies in the range  $1 \text{ TeV} < \sqrt{s} < 5 \text{ TeV}$ , with a luminosity of  $10^{35} \text{ cm}^{-2} \text{ s}^{-1}$  at  $\sqrt{s} = 3 \text{ TeV}$ , based on the two-beam acceleration scheme [1]. While opening a new domain for experimentation at  $e^+e^-$  colliders, CLIC also presents new challenges compared to any other linear collider project, due to its different regime of operation, thus requiring a significant effort in the optimisation of its parameters and assessing the implications of the machine induced backgrounds on its physics potential.

The definition of its physics programme still requires essential data that is likely to become available only after the first years of LHC operation and, possibly, also the results from a lower energy linear collider such as TESLA [2]. At present we have to envisage several possible scenarios for the fundamental questions to be addressed by HEP experiments in the second decade of the new century.

In this note a set of benchmark physics signatures for the optimisation of the CLIC parameters are proposed. Each of these signatures may signal the manifestation of different scenarios of new physics, possibly beyond those that we are able to define today. The optimisation of the machine design and the study of its potential for each of them will also guarantee a more general applicability to other processes, characterised by similar topologies.

Furthermore, while considering experimentation at a multi-TeV collider, it is interesting to verify to which extent extrapolations of the experimental techniques, successfully developed at LEP and being refined in the studies for the TESLA project, are still applicable. This has important consequences on the requirements for the experimental conditions at the CLIC interaction region and for the definition of the CLIC physics potential.

## 2 Physics Signatures

These considerations have motivated a preliminary investigation of physics signatures at CLIC that are characteristic of one or more physics scenarios of interest and relevant to specific aspects of the accelerator performances and/or of the detector response. Four physics signatures have been identified:

1. Resonance Scan
2. Electro-weak Fits
3. Multi-Jet Final States
4. Missing Energy and Forward Processes

In the following, these are discussed in some details on the basis of the first results of dedicated simulations of several relevant physics processes. The cross sections have been estimated using the COMPHEP program [3] and the simulated events generated using the PYTHIA-6 Monte Carlo [4] (see Figure 1). Events

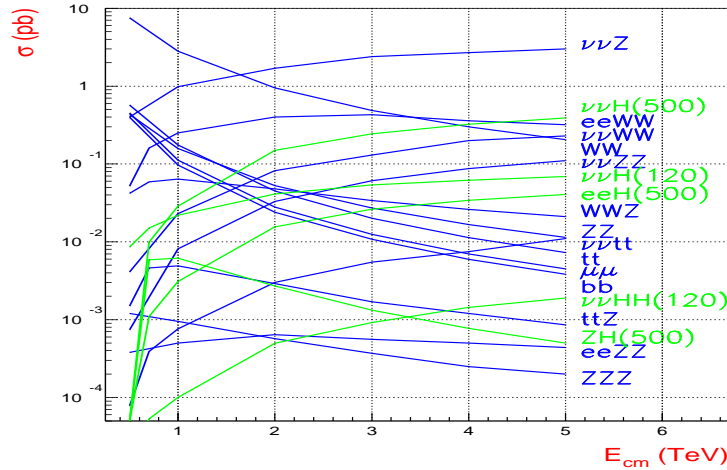


Figure 1: Cross sections for SM processes at  $\sqrt{s} = 1-5$  TeV.

have been passed through either a parametric smearing using the SIMDET program [5] or a full GEANT-3 [6] based simulation. In both cases the detector design and its performances have been assumed to correspond to those of the detector designed for the TESLA linear collider Conceptual Design Report [2]. In view of the different energy and backgrounds here considered for CLIC, the strength of the magnetic field and the radius of the detector layer closer to the beam pipe have been changed from 3 T to 4-6 T and from 1.5 cm to  $\simeq 3.0$  cm respectively. The expected luminosity spectrum and  $\gamma\gamma$  background have been

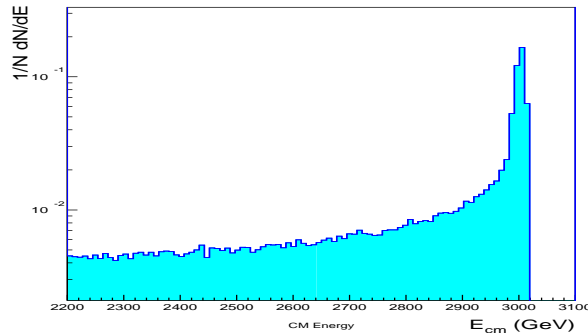


Figure 2: The upper portion of the CLIC luminosity spectrum at  $\sqrt{s} \simeq 3$  TeV.

obtained from the GUINEAPIG simulation, with the CLIC reference parameters at  $\sqrt{s} = 3$  TeV [7], and interfaced to PYTHIA with the CALYPSO and HADES programs respectively [8].

## 2.1 Resonance Scan

The most striking manifestation of new physics in the multi-TeV region will come from the sudden increase of the  $e^+e^- \rightarrow f\bar{f}$  cross section signalling the s-channel production of a new particle. There are several scenarios predicting new resonances in the mass range of interests for CLIC. The first one is the existence of extra gauge bosons such as a  $Z'$  boson. This is common to both GUT-inspired  $E_6$  models and to Left-Right symmetric models. A  $Z'$  boson within the kinematical reach of CLIC should be already observable at the LHC and CLIC will concentrate on the accurate measurements of its properties by a direct resonance scan and by the electro-weak fits discussed in the next section. It is interesting to note that a recent re-analysis of data on atomic parity violation shows that the observed  $2.8\sigma$  deviation from the SM prediction [9] can be explained by a  $Z'$  boson with mass in the range  $0.6 \text{ TeV}/c^2 < M(Z') < 1.5 \text{ TeV}/c^2$  that is compatible with the present limits [10].

New resonances are also predicted by new theories of gravity with extra dimensions in the form of Kaluza-Klein graviton and gauge boson excitations. Their phenomenology at the TeV scale has been analysed [11, 12] and the results can be extended to the case of the CLIC multi-TeV collider. Models of dynamical electro-weak symmetry breaking also predict the existence of new resonances in the TeV region. In particular the degenerate BESS model introduces a pair of narrow and nearly degenerate vector and an axial-vector resonances [13]. The study of such resonances will have to establish their nature, to accurately determine their mass and width and to disentangle a wide resonance from the superposition of two nearly degenerate states.

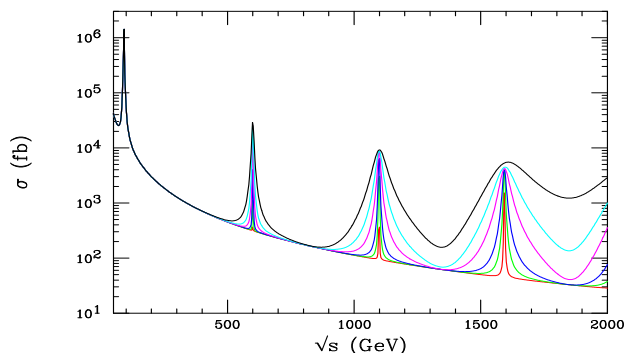


Figure 3:  $\sigma(e^+e^- \rightarrow \mu^+\mu^-)$  vs.  $\sqrt{s}$  for a fixed spectrum of KK resonances with different width  $\Gamma_{KK} = f(c)M_{KK}^3$  in the RS model [14] (from [11]).

Most relevant to the resonance scan signature are the characteristics of the luminosity spectrum and the ability to perform jet flavour identification.

A preliminary study of on-shell  $Z'$  production at CLIC has been performed already based on parametric smearing.  $e^+e^- \rightarrow Z'$  events have been generated for

$M(Z') = 3.0 \text{ TeV}/c^2$  including ISR, beam energy spectrum and  $\gamma\gamma$  backgrounds assuming SM-like couplings, corresponding to a width  $\Gamma_{Z'} \simeq 90 \text{ GeV}/c^2$ . Due to the large signal cross-section over a flat background and the large CLIC luminosity, a precise study of the mass, width and couplings can be performed. The mass and width of resonance can be determined by performing either an energy scan, like the  $Z^0$  scan performed at LEP/SLC and foreseen for the  $t\bar{t}$  threshold, or an auto-scan, by tuning the collision energy just beyond the top of the resonance and profiting of the long tail of the luminosity spectrum to probe the resonance peak. For the first method both di-jet and di-lepton final states can be considered, while for the auto-scan only  $\mu^+\mu^-$  final states may provide with the necessary accuracy for the  $Z'$  energy. Preliminary results are shown in Figure 4. Assuming an integrated luminosity of  $1000 \text{ fb}^{-1}$ , corresponding to one year of CLIC running at its nominal luminosity, a relative statistical accuracy of  $\pm 5 \times 10^{-5}$  for the mass and of  $\pm 3 \times 10^{-3}$  for the total width can be obtained.

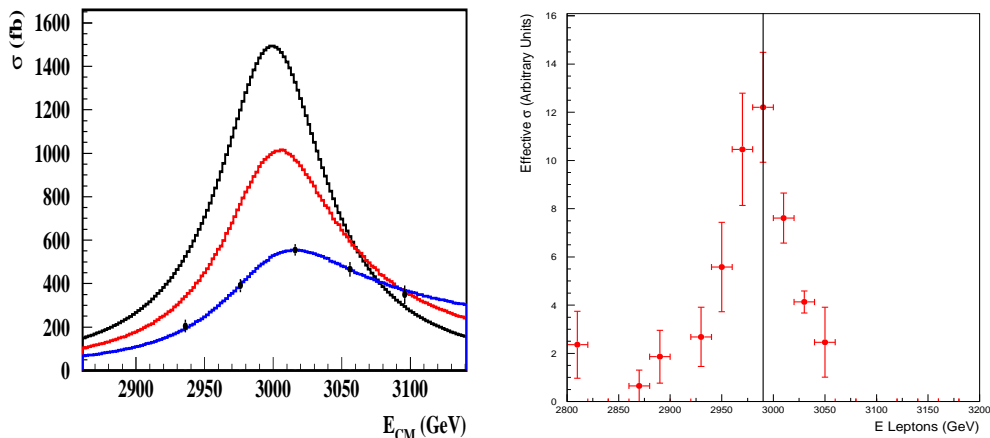


Figure 4: *The  $Z'$  resonance scan obtained with energy scan (left) and auto-scan (right). In the left plot, the Born production cross-section, the cross section with ISR included and that accounting for the luminosity spectrum and the tagging criteria are shown.*

## 2.2 Electro-weak Fits

If a new resonance, such as a  $Z'$ , will have been found at the LHC or at a lower energy linear collider, the CLIC physics programme will be largely focused on the precise study of its nature via the measurement of its fundamental properties. This will closely follow the LEP physics programme at the  $Z^0$  peak. The main issue in these studies will be the determination of the nature of the observed resonance. A precise study of its couplings to up- and down-type quarks and of forward-backward asymmetries may be instrumental in this program. As an example, the nearly degenerate Kaluza-Klein excitations of the  $Z$  and  $\gamma$  [15] or

the  $L_3$  and  $R_3$  resonances of the BESS model need to be distinguished from a  $Z'$  boson.

Even if such a resonance is not found, precise electro-weak data for  $\sigma(e^+e^- \rightarrow f\bar{f})$ ,  $A_{FB}^{f\bar{f}}$  and  $A_{LR}^{f\bar{f}}$  (with  $f\bar{f} = \ell^+\ell^-$ ,  $c\bar{c}$ ,  $b\bar{b}$ ,  $t\bar{t}$ ) at  $\sqrt{s} = 1 - 5$  TeV may give indirect evidence of new phenomena such as an heavier  $Z'$  well beyond the CLIC kinematical limit, extra-dimensions or contact interactions. It is therefore important to ensure that accurate electro-weak data can be obtained.

The main experimental requirements highlighted by electro-weak fits are the identification of the  $e^+e^- \rightarrow f\bar{f}$  from  $\gamma\gamma \rightarrow$  hadrons final states, the ability to reconstruct and tag the fermions down to small polar angles, in presence of a significant  $\gamma\gamma \rightarrow$  hadrons background, the reconstruction of the colliding  $e^+e^-$  rest frame in presence of large beamstrahlung and the possibility to obtain highly polarised  $e^-$  and  $e^+$  beams.

Good examples of the CLIC potential are given by the sensitivity to a heavy  $Z'$  and to extra-dimensions. Direct or indirect evidence of an additional neutral gauge boson will require a detailed study of its couplings to determine the underlying extended gauge structure. Extrapolating the results of a previous study on extra dimensions based on the forward-backward asymmetry  $A_{fb}$  in  $e^+e^- \rightarrow b\bar{b}$  [16], the CLIC sensitivity for  $M_S$ , representing the scale at which gravity becomes strong, is given by  $\simeq 7 \times \sqrt{s}$  (TeV) if the  $b\bar{b}$  final state can be identified efficiently.

Table 1:  $b\bar{b}$  production cross-section from  $\sqrt{s} = M(Z^0)$  up to 3 TeV.

$\sqrt{s}$ (TeV)	0.09	0.5	0.8	<b>3.0</b>
$\sigma_{b\bar{b}}$ (pb)	9160	0.4	0.15	<b>0.012</b>
$\int L$		500 pb $^{-1}$	500 pb $^{-1}$	<b>5000 fb<math>^{-1}</math></b>
$N_{b\bar{b}}$	900k	200k	75k	<b>60k</b>

Therefore, the identification of  $b\bar{b}$  and  $c\bar{c}$  final states represents an important benchmark process also at CLIC. At 3 TeV  $\sigma(e^+e^- \rightarrow b\bar{b})$  is only of the order of 0.01 pb but the heavy hadrons receive a significant boost to acquire decay distances in space of several centimetres, i.e. an order of magnitude larger compared to those at LEP energies. This has important experimental consequences. The long decay distance of  $B$  hadrons, exceeding the anticipated radii of the first layers of the Vertex Tracker, suggests a tagging algorithm based on the topological tag of secondary vertices rather than on large track impact parameters as performed at LEP. A beauty tag based on the change in charged multiplicity detected through the layers of a Si Vertex Tracker, that applies to CLIC a concept originally developed in charm photo-production experiments [17], has been proposed [18]. Such a tag can be part of the track pattern recognition that still needs

Table 2: Average decay distance in space for  $B$  hadrons at different  $\sqrt{s}$

$\sqrt{s}$ (TeV)	0.09	0.2	0.35	0.5	<b>3.0</b>	
Process	$Z^0$	$HZ$	$HZ$	$HZ$	$H^+H^-$   $bb$	
$d_{space}$ (cm)	0.3	0.3	0.7	0.85	<b>2.5</b>	<b>9.0</b>

to be studied in full details in the challenging environment produced by the high jet collimation and background hits from pair and  $\gamma\gamma \rightarrow$  hadrons production. This represents an important benchmark for the design of the vertex and main trackers. Different silicon pixel technologies have been proposed for the Vertex Tracker at TESLA and NLC [19]. Assuming a 25 ns time stamping capability, such as for the LHC hybrid pixel sensors, the Vertex Tracker integrates about 30 bunch crossing corresponding to an hit density due to pairs of  $\simeq 0.17 \text{ mm}^{-1}$  at 3.0 cm that becomes  $\simeq 0.8 \text{ mm}^{-1}$  if the full train of 154 bunches is integrated [7]. These rates appear to be manageable for a Vertex Tracker with redundant radial measurements and small enough cell size.

The resolution for extrapolating a particle track to its production point has been estimated assuming the first sensitive layer at 3.0 cm radius, a single point resolution of  $8 \mu\text{m}$  and  $250 \mu\text{m}$  sensor thickness that represent realistic assumptions for a Vertex Tracker based on hybrid pixel sensors [19]. The result is shown in Figure 5 as a function of the particle momentum.

### 2.3 Multi-Jet Final States

Multi-jet final states are a common signature for many physics processes from heavy Higgs pair production to  $WW$  scattering. Evolving from the  $Z^0$  peak to multi-TeV c.m. collisions, the number of jets increases due to gluon radiation and the crossing of thresholds for multi-fermion final state production.

Table 3: Average reconstructed jet multiplicity in hadronic events at different  $\sqrt{s}$  energies.

$\sqrt{s}$ (TeV)	0.09	0.20	0.5	0.8	3.0	5.0
$\langle N_{Jets} \rangle$	2.8	4.2	4.8	5.3	6.4	6.7

There are several physics processes of possible interest at CLIC energies characterised by multi-jet final states. In the Higgs sector, the reconstruction of the Higgs potential, requiring the determination of the triple and quartic Higgs couplings through the measurement of double and triple Higgs production diagrams,

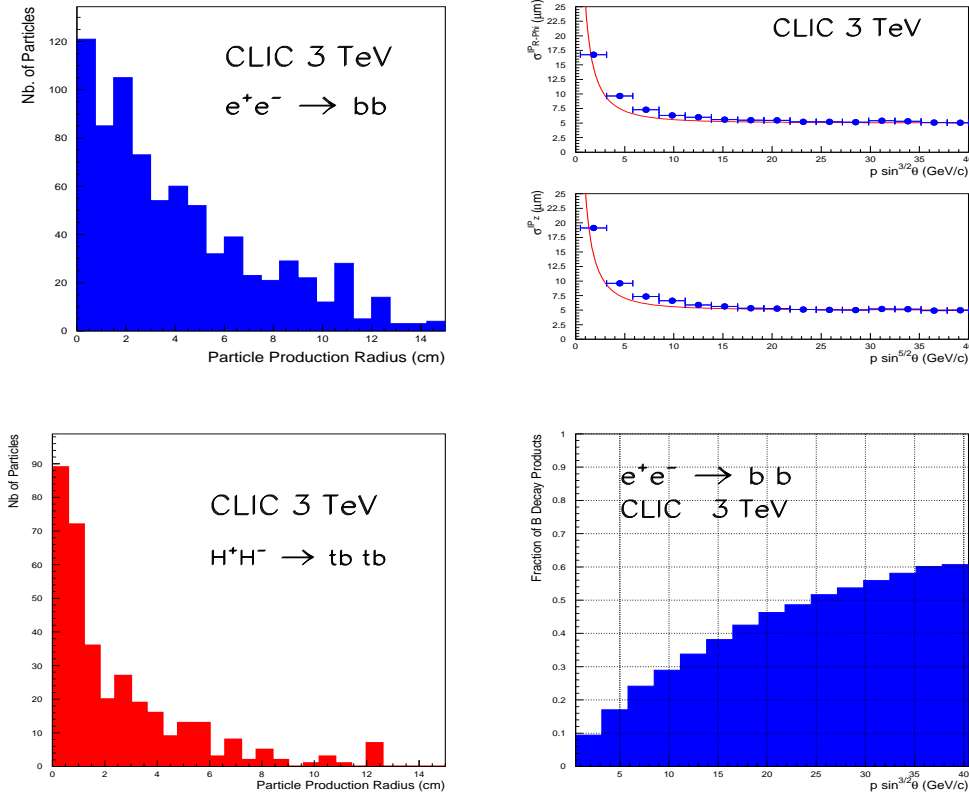


Figure 5: Distributions of the decay distances for  $B$  hadrons produced in  $e^+e^- \rightarrow b\bar{b}$  (upper left) and  $e^+e^- \rightarrow H^+H^- \rightarrow t\bar{t}b\bar{b}$  decays (lower left), impact parameter resolution expected for a Vertex Tracker at CLIC plotted as a function of the particle momentum (upper right) and fraction of secondary particles with momentum below a given value (upper left) in  $b\bar{b}$  events.

and the study of the Higgs Top-Yukawa coupling will be required to complete the Higgs profile investigation and as proof of the Higgs mechanism of mass generation. The small values of the cross sections for these processes will require the large collision energies and integrated luminosities that can be achieved at CLIC [20]. Even for a Higgs boson as light as  $120 \text{ GeV}/c^2$ , the  $e^+e^- \rightarrow \nu_e\bar{\nu}_e HH$  cross section is only  $0.05 \text{ fb}$  at  $\sqrt{s} = 0.8 \text{ TeV}$  and becomes  $0.92 \text{ fb}$  at  $\sqrt{s} = 3.0 \text{ TeV}$ . The triple Higgs production is suppressed by a factor of  $\simeq 10^3$ . CLIC could produce enough of these events for the triple Higgs couplings to be determined to better than 10% and to obtain also information on the elusive quartic coupling.

As another example, the heavy Higgs sector in SUSY models may require a multi-TeV collider for accessing  $e^+e^- \rightarrow H^+H^-$  and  $H^0A^0$  pair production. As indicated in Table 4, these processes are characterised by large jet multiplicities that need to be properly handled in order to isolate the small expected signals. Multi-jet final states probe the detector performance in terms of two particle



Table 4: Examples of Higgs processes with large jet multiplicity.

Process	$\sigma$ (fb)	$M_H$ (GeV/ $c^2$ )	Events / 5000 fb $^{-1}$	$N_{Jets}$
$t\bar{t}H \rightarrow WW/ZZ (t\bar{t})$	0.18	500	850	10 (12)
$ZHH \rightarrow WW/ZZ (t\bar{t})$	0.038	500	190	10 (14)
$\nu\bar{\nu}HH \rightarrow WW/ZZ$	0.062	500	310	8 (12)
$ZHH \rightarrow b\bar{b}$	0.036	120	180	6
$\nu\bar{\nu}HH \rightarrow b\bar{b}$	0.94	120	4700	4
$H^+H^- \rightarrow t\bar{t}$	2.0	800	10000	8

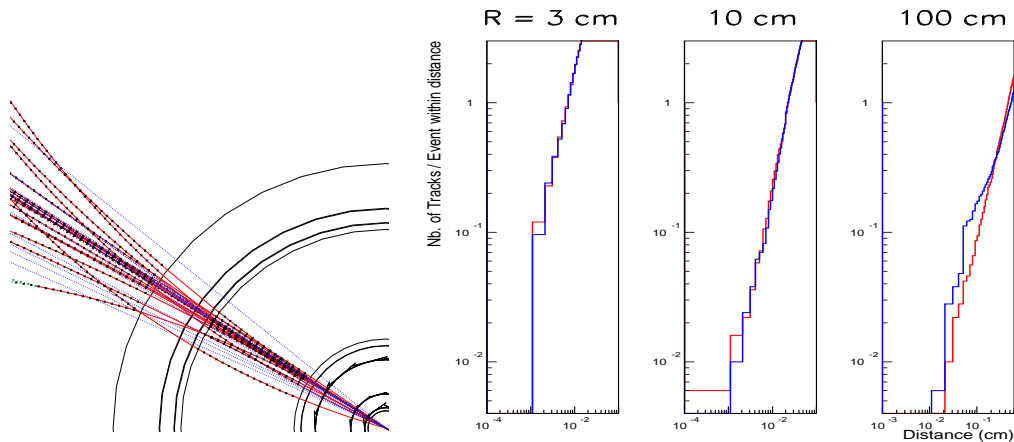


Figure 6: Magnified view of a di-jet from a  $e^+e^- \rightarrow W^+W^-$  event at  $\sqrt{s} = 3$  TeV (left) and the distance from the closest track for charged particle with  $p > 3$  GeV/ $c$  at different radial distances (right) for  $B = 4$  T (dark grey histogram) and 6 T (light grey histogram).

separation and energy flow, while the broad luminosity spectrum represents a source of inaccuracy when performing constrained fits and the large  $\gamma\gamma \rightarrow$  hadrons background expected at CLIC may confuse the topological event reconstruction adding or smearing jets in the forward regions.

The anticipated large jet multiplicity and boost make it necessary to reconsider the definition of jet clustering, intra-jet and inter-jet particles. In particular for processes like  $e^+e^- \rightarrow W^+W^-$ , with a cross-section of 0.5 pb at  $\sqrt{s} = 3$  TeV, the jet collimation may make the resolution of the individual charged and neutral particles problematic. Figure 6 shows the distance from the closest track for a charged particle with  $p > 3$  GeV/ $c$  at different radial distances from the interaction point, while Figure 7 shows the energy flow at the entrance of a calorimeter located at a radius of 170 cm for a typical  $W^+W^-$  hadronic decay.

These considerations seem to favour an inclusive approach where hadronic

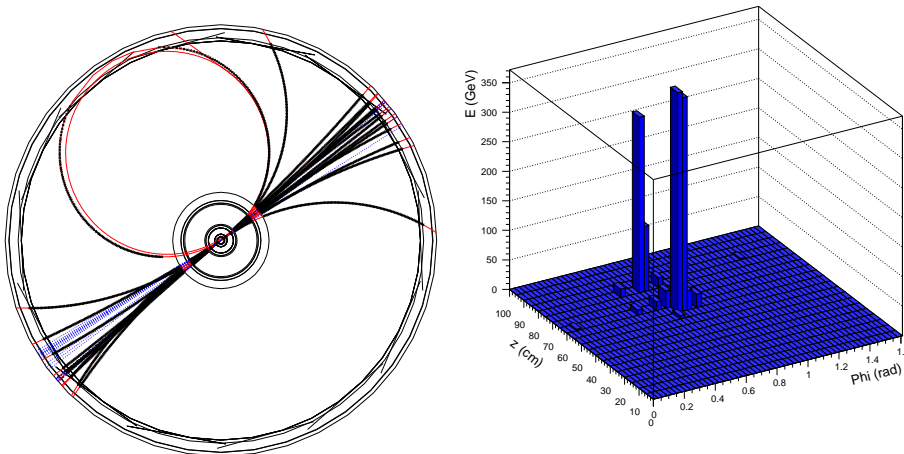


Figure 7: A  $e^+e^- \rightarrow W^+W^-$  event at  $\sqrt{s} = 3$  TeV (left) and the energy flowing at the entrance of the e.m. calorimeter located at a radius of 170 cm assuming a solenoidal field of 6 T and  $5 \times 5$  cm<sup>2</sup> cell size (right).

jets are reconstructed as elementary objects in the calorimeters. On the other hand, jet pairing ambiguity in channels with large jet multiplicity and heavy quark identification make jet flavour and charge identification highly important in order to suppress the combinatorial and multi-fermion backgrounds. This in turn requires efficient and accurate tracking capabilities in collimated hadronic jets.

## 2.4 Missing Energy and Forward Processes

The detector ability to identify events with large missing energy is an important requisite since this is the main signature for production and decay of supersymmetric particles, such as  $\tilde{\ell}^+\tilde{\ell}^-$  and  $\tilde{\chi}^+\tilde{\chi}^-$ , and a possible complement in the study of the Higgs sector through invisible decays. In particular the search for  $e^+e^- \rightarrow \tilde{\ell}^+\tilde{\ell}^-$  at  $\sqrt{s} > 1$  TeV will fully cover the region of the  $(m_{1/2}, m_0)$  MSSM parameter plane preferred by the LSP cosmological relic density [21].

Processes whose production cross section is peaked in the forward region, such as Higgs production in  $WW$  and  $ZZ$  fusion, are also important and their observability must be guaranteed. Finally, the study of  $W^+W^- \rightarrow W^+W^-$  and  $W^+W^- \rightarrow Z^0Z^0$  cross sections probes the possible dynamics of strong electro-weak symmetry breaking at  $\sqrt{s} > 1$  TeV [22]. In order to ensure an efficient rejection of the  $e^+e^-W^+W^-$  and  $e^\pm\nu W^\pm Z^0$  backgrounds, electron detection capabilities must be ensured down to small polar angles.

These requisites have to be verified against the significant  $\gamma\gamma$  background that limits the event reconstruction at small angles. The effect of the  $\gamma\gamma$  background has been studied by tracking the  $\gamma\gamma \rightarrow$  hadrons products using the full GEANT simulation and recording the measured  $E$  and  $E_T$  assuming a detector polar

### CLIC 3 TeV

$$e^+e^- \rightarrow e_L e_R$$

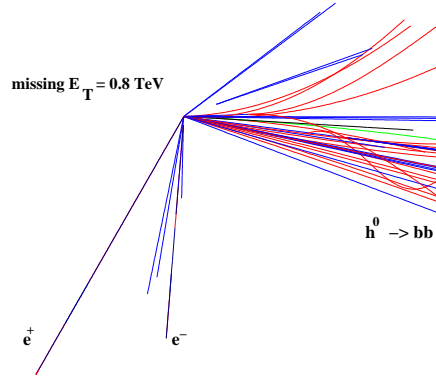


Figure 8: Event display of a  $e^+e^- \rightarrow \tilde{e}_L \tilde{e}_R$  reaction followed by the cascade decays  $\tilde{e}_R \rightarrow e\chi_1^0$ ,  $\tilde{e}_L \rightarrow e\chi_2^0$ ,  $\chi_2^0 \rightarrow h\chi_1^0$ ,  $h \rightarrow b\bar{b}$  for selectron masses of 1050 GeV and  $m_h = 115 \text{ GeV}/c^2$ .

angle coverage down to 150 or 80 mrad. The results are shown in Figure 9. It is observed that, while the energy deposition is very significant, the observed transverse energy is limited at about 100 GeV.

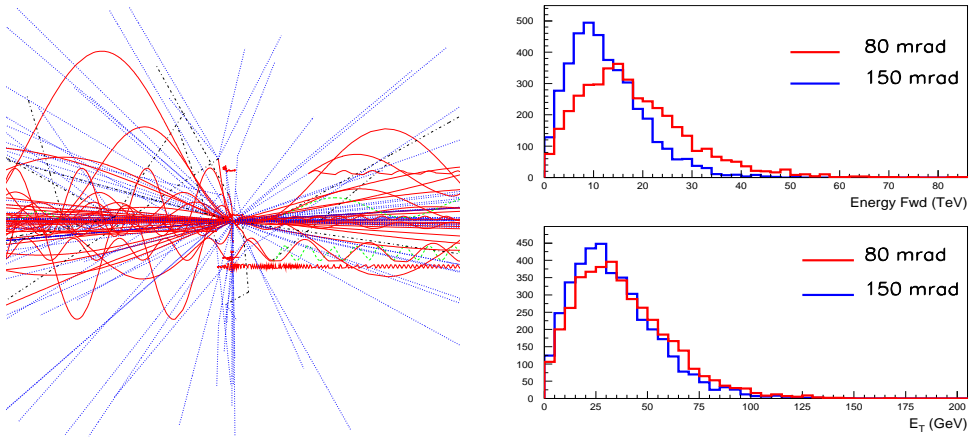


Figure 9: Event display (left) and  $E$  and  $E_T$  distributions (right) for the  $\gamma\gamma$  background events generated in a single CLIC bunch crossing for different detector polar angle coverages.

Higgs production via  $ZZ$  fusion in the process  $e^+e^- \rightarrow H^0 e^+e^-$  has been investigated for  $M_H = 600 \text{ GeV}/c^2$ . At high  $\sqrt{s}$  and large values of the Higgs mass the  $ZZ$  fusion process is favourable to study an exotic or invisibly decaying Higgs. If the  $e^+e^-$  in the final state can be tagged, this process allows to identify

Higgs decays by the recoil mass independently of the Higgs decay modes and benefits of a production cross section of 30 fb to 15 fb for Higgs masses in the range  $400 \text{ GeV}/c^2$  to  $900 \text{ GeV}/c^2$  compared to  $\simeq 1.5 \text{ fb}$  for the Higgs-strahlung  $HZ$  process. Figure 10 shows the production polar angle for the electron and positron peaking at  $\simeq 50 \text{ mrad}$ . Assuming tagging and tracking capabilities extending to  $120 \text{ mrad}$ , for electron with energy exceeding  $700 \text{ GeV}$ , the  $e^+e^-$  recoil mass can be used to isolate the Higgs signal also when accounting for the mass peak broadening due to the luminosity spectrum.

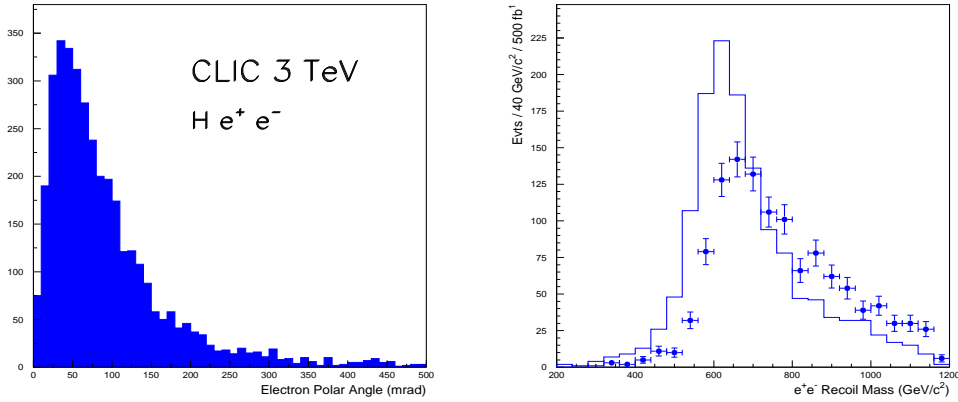


Figure 10: Polar angle distribution for electrons (left) and  $ee$  recoil mass spectrum in the  $ZZ$  fusion reaction  $e^+e^- \rightarrow H^0e^+e^-$  for  $\sqrt{s} = 3 \text{ TeV}$  and  $M_H = 600 \text{ GeV}/c^2$ . The histogram (points with error bars) show the distribution before (after) accounting for the luminosity spectrum and  $\gamma\gamma$  background.

### 3 Conclusions

A first survey of signatures for physics processes of potential interests at the CLIC  $e^+e^-$  linear collider at  $\sqrt{s} \simeq 3 \text{ TeV}$  has been performed. Four physics signatures have been identified: i) Resonance Scan, ii) Electro-weak Fits, iii) Multi-Jet Final States and iv) Missing Energy and Forward Processes and examples of reference reactions have been identified to test the effect of the accelerator parameters and of the detector response on the CLIC physics potential.

### Acknowledgements

I am grateful to S. De Curtis, D. Dominici, J. Ellis, A. De Roeck, G. Guignard, D. Schulte, R. Settles, D. Treille and G. Wilson for ideas and suggestions on several topics discussed in this note.

Table 5: *Physics Signatures and CLIC Physics Program*

Physics Signatures	Higgs Sector	SUSY	SSB	New Gauge Bosons	Extra Dimensions
Resonance Scan		SUSY Thresholds	D-BESS	$Z'$	KK
EW Fits				$A_{LR}, A_{FB}$	$A_{FB}^{b\bar{b}}$
Multi-Jets	$H^+H^-$ $t\bar{t}H$ $HH\nu\bar{\nu}$ $HHZ$ $HHH\nu\bar{\nu}$ $HHHZ$		Techni- $\rho$		
$E_{miss}$ , Fwd	$He^+e^-$	$\tilde{\ell}^+\tilde{\ell}^-$ $\tilde{\chi}^+\tilde{\chi}^-$	WW scattering		

Table 6: *Physics Signatures and CLIC Parameters: Benchmarks and Challenges*

Physics Signatures	Beam-Strahlung	Beam $E$ Spread	$e^+$ Polarisation	Pairs	$\gamma\gamma$ Bkg.
Resonance Scan	Stat. Shape Syst.	Shape Syst.	Couplings	$\Gamma_{bb,cc,tt}$	$\Gamma_{bb,cc,tt}$
EW Fits	Unfold Boost		Polarisation Measurement	$bb, c\bar{c}$ Tags	$\cos\theta_{min}$ Bkg Flavour
Multi-Jets	5-C Fit			Tags for Jet pairing	Fake Jets
$E_{miss}$ Fwd	$\theta_{miss}$			Fwd Tracking	$E_{hem}$ $E_T$

## References

- [1] *A 3 TeV  $e^+e^-$  Linear Collider Based on CLIC Technology*, G. Guignard (editor), CERN-2000-008.
- [2] *Conceptual Design of a 500 GeV  $e^+e^-$  Linear Collider with Integrated X-ray Laser Facility* R. Brinkmann, G. Materlik, J. Rossbach and A. Wagner (editors), DESY 1997-048 and ECFA 1997-182.
- [3] A. Pukhov *et al.*, *CompHEP - a package for evaluation of Feynman diagrams and integration over multi-particle phase space*, hep-ph/9908288.
- [4] T. Sjöstrand, *Comp. Phys. Comm.* **82** (1994), 74 and update in <http://www.thep.lu.se/~torbjorn/pythia/pythia6150.update>.
- [5] M. Pohl and J. Schreiber, *SIMDET - A Parametric Monte Carlo for a TESLA Detector*, DESY 99-030.
- [6] *GEANT - Detector Description and Simulation Tool*, CERN Program Library Long Writeup W5013 (1994).
- [7] D. Schulte, in *Proc. of the Workshop on future linear electron-positron colliders for particle physics and for research using free electron lasers*, Lund (Sweden), Sept. 1999, 59.
- [8] The GUINEAPIG, CALYPSO and HADES programs are by D. Schulte.
- [9] S.C. Bennet and C.W. Wiemann, *Phys. Rev. Lett.* **82** (1999), 2484.
- [10] R. Casalbuoni *et al.*, *Z' indication from new APV data in Cesium and searches at linear colliders*, LC-TH-2000-006 and hep-ph/0001215.
- [11] T.G. Rizzo, in *Proc. of the 3<sup>rd</sup> Int. Workshop on  $e^-e^-$  Interactions at TeV Energies*, Santa Cruz, CA, Dec. 1999 and SLAC-PUB-8339.
- [12] T.G. Rizzo, *Randall-Sundrum Phenomenology at Linear Colliders*, SLAC-PUB-8703 and hep-ph/0011139.
- [13] R. Casalbuoni *et al.*, *Phys. Rev.* **D56** (1997), 5731.
- [14] L. Randall and R. Sundrum, *Phys. Rev. Lett.* **83** (1999), 4690.
- [15] T.G. Rizzo, *Phys. Rev.* **D61** (2000), 055005.
- [16] J.L. Hewett, *Phys. Rev. Lett.* **82** (1998) 4765.
- [17] A. Albini *et al.* (NA1 Collaboration), *Phys. Lett.* **B 110** (1982), 339.

- [18] M. Battaglia, to appear in the Proc. of the *9<sup>th</sup> Int. Workshop on Vertex Detectors - Vertex2000*, Homestead, MI (USA), September 2000.
- [19] M. Battaglia and M. Caccia, in *Proc. of the Workshop on future linear electron-positron colliders for particle physics and for research using free electron lasers*, Lund (Sweden), Sept. 1999, 273 and hep-ex/9911039.
- [20] A. Djouadi *et al.*, *Eur. Phys. J.* **C10** (1999) 27.
- [21] J. Ellis *et al.*, *Phys. Lett.* **B 474** (2000) 314.
- [22] V. Barger *et al.*, *Phys. Rev.* **D 52** (1995), 3815.